APPLICATION OF A NOVEL FUZZY LOGIC CONTROL IN SOLAR PV POWERED MODULAR MULTILEVEL INVERTER FOR MARINE WATER PUMPING AREAS

[1]MR.M.SURYAKANTH, [2]PUTTAPAKA SAI KUMAR, [3]PEDDAPALLY DINESH, [4]MADIGA RAHUL

[1](Assistant professor), EEE. Guru Nanak Institutions Technical Campus, Hyderabad.

[234]B.Tech Scholars, EEE. Guru Nanak Institutions Technical Campus, Hyderabad.

ABSTRACT

On ships, marine water pumping is essential for many tasks; it uses around half of the energy used overall and poses several difficulties. Conventional maritime power systems, which mostly use diesel engines, contribute to air pollution and emissions by releasing 2.8% of carbon dioxide (CO2), 15% of nitrogen oxides (NOX), and 13% of sulfur oxides (SOX). Nonetheless, the need of switching to greener and more sustainable energy sources for maritime applications is becoming more apparent. The existing maritime power systems, which mostly depend on diesel engines, encounter many obstacles including worries about energy security and the consequences of greenhouse gas emissions on the environment. The proposed project would combine a modular multilevel inverter (MMI) with solar photovoltaic (PV) technology to overcome these issues. The suggested system seeks to lower air emissions and energy consumption related to marine water pumping by employing clean and sustainable solar power. Energy efficiency will be maximized in large part by the MMI's capacity to regulate the speed of an Induction Motor (IM) drive powered by solar photovoltaics. Furthermore, accurate speed management of the induction motor will be ensured by the integration of controllers based on fuzzy logic controllers (FLC) and proportional-integral (PI), improving overall system performance and power quality. The eleven-level inverter that is being developed will be able to regulate the speed of an IM drive that is powered by solar photovoltaics. To improve performance, PI and FLC based controllers will be included into the inverter analysis process. The appropriateness of the system for a water pumping system designed for maritime applications is investigated by means of a comparative analysis technique that looks at both the steady state and dynamic behaviors. By using MATLAB/SIMULINK, it will be possible to demonstrate and analyze the behavior of the FLC-based control and simulate results. These outcomes will be used to assess controller performance, inverter output voltage improvement, dependable induction motor speed control, and power quality, especially with regard to harmonics.

1. INTRODUCTION

1.1 General

Globally, the shipping and marine sectors are making significant efforts to lower the amount of energy used and emissions into the atmosphere. The International Convention for the Prevention of Pollution from Ships organization (MARPOL) has established severe guidelines for the deterrence of pollution in the maritime environment and unintentional causes [1], [2]. Shipping contributes around 3% of the world's CO2 emissions from diesel engines used in the maritime industry, which is a result of climate change and greenhouse gas emissions [3]. 2.8% of carbon dioxide (CO2), 15% of nitrogen oxides (NOX), and 13% of sulfur dioxide (SO2) are released by marine cargo diesel engines.

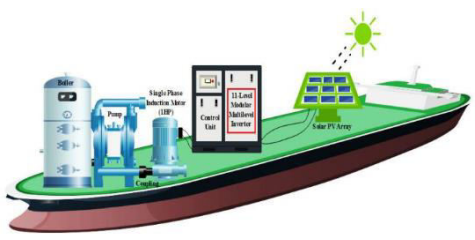

Fig 1.1 Schematic diagram of the proposed 11-level inverter.

The primary gases that cause the greatest atmospheric pollution are sulphur oxides (SOx). The International Maritime Organization (IMO) and the United Nations Framework Convention on Climate Change (UNFCCC) conducted in-depth studies and developed guidelines and policies for the shipping sector's reduction of CO2 emissions. The depletion of traditional energy sources is not the only factor contributing to the developing global energy problem; air and water pollution is also a major factor. The use of diesel engines in ships results in the progressive growth of greenhouse gas emissions, which reached 8% in 2020.

For the majority of suburban and maritime applications, solar power is often the best option since it needs less maintenance, operates silently because it doesn't have any moving components, and takes up less space on ship roofs. The ship's solar photovoltaic energy system is used to provide the necessary electricity and uses a cutting-edge method to reduce emissions, increasing the efficiency of renewable energy sources and enhancing power stability. To interact with various high-power loads, the solar energy source is combined with an inverter and power electronic converter [6]. Recently, a broad variety of research has been conducted on the relationship between integrated power converters for renewable energy and contemporary ships. Voltage variation and frequency deviation, which cause harmonic distortions, are the two main problems that arise in power converters [7], [8]. About 70% of the ship's total electrical energy is used by the pumping systems [9], [10]. A crucial component of ship power electronics, converters are utilized to power motor driving systems but are severely impacted by harmonic setbacks.

The proposed study looks at the latest advancements in modular inverters, which are used in ships to reduce harmonics with the help of an intelligent controller and therefore enhance power quality. In order to produce negative voltage levels, the study offers a unique symmetric multilevel module based on the cascade category that does not need the use of an extra circuit. Figure 1 depicts a solar-fed eleven-level inverter with sophisticated control approaches intended to achieve better performance parameters for maritime applications. The seawater cooling pump located on the ship is powered by a variable frequency motor that is powered by the inverter. Using PI and FLC based controllers, the multilevel inverter fed IM drive's performance is evaluated. Most speed control applications employ the proportional-integral (PI) controller because of its superior maximum peak overshoot and stability.

When it comes to clever controllers for induction motor speed control applications, the FLC is the most straightforward model.

The ship's water is constantly pumped from dawn to dusk. Therefore, it is necessary to regulate the inverter in order to maintain the beginning current and fixed voltage of an induction motor.

Commutation issues arise with conventional DC motors. Within the ship, induction motors are greatly sought as a means of overcoming the drawbacks of DC motors. The fresh water is properly cooled by the ocean, which pumps enough. The single phase IM drive for marine water pumping that is used in sustained control systems with MMI topology is the subject of the proposed research project [11].

The maximal solar power extraction under the atmospheric circumstances controls the real-time speed control implementation. In addition, the inverter progressively modifies the switching frequency in order to regulate the speed of an induction motor. This is accomplished by the optimum Pulse Width Modulation (PWM), which is produced for a FL controller to improve the power quality with the help of a modulating signal. In order to improve system performance overall, the simulation research focuses on designing a solar PV fed MMI that powers an IM drive using PI and FL based controllers. The SPARTAN3E500 FPGA controller, used in the development of the prototype model, produces the pulses required by the system's inverter and converter. The following examples show the contributions made in the paper:

Examining how well PI and FL based controllers work with the IM drive system for marine water pumping; Using the SPARTAN3E500 FPGA controller to implement an MMI fed IM drive in real time; and Comparing the effectiveness of FL and PI based controllers to improve power quality The performance analysis of MMI is the primary subject of this research.

The paper is formulated as follows: Section V describes the experimental setup and discussions, Section II presents the system configuration and operation strategy, Section III describes the control technique for the suggested topology, and Section IV analyzes the simulation findings.

1.2 SOLAR PHOTOVOLTAICS

1.2.1 Introduction

Becquerel was the first to notice the photovoltaic effect, which converts solar energy. It is usually understood to mean that when light is shone on a solid or liquid system, an electric voltage appears between two electrodes linked to the system. Solar cells are energy conversion devices that employ the photovoltaic effect to transform sunlight into electrical current. A solar cell, or more broadly a photovoltaic cell, is a single converter cell. A solar array, or solar module, is a group of these cells intended to maximize the generation of electric power; this is how the term "photovoltaic arrays" originates. Solar cells may be grouped together in enormous configurations known as arrays. These arrays, which are made up of thousands of individual cells, may serve as central power plants that distribute electrical energy produced by sunlight to consumers in the commercial, residential, and industrial sectors. Solar cell panels, or just panels, are the popular term for solar cells in considerably smaller shapes. Almost every photovoltaic device has a P-N junction in a semiconductor, which is used to create the photovoltaic voltage. Semiconductor material, mostly silicon, makes up the solar panels' basic composition.

1.2.2 Basics of Solar Cells

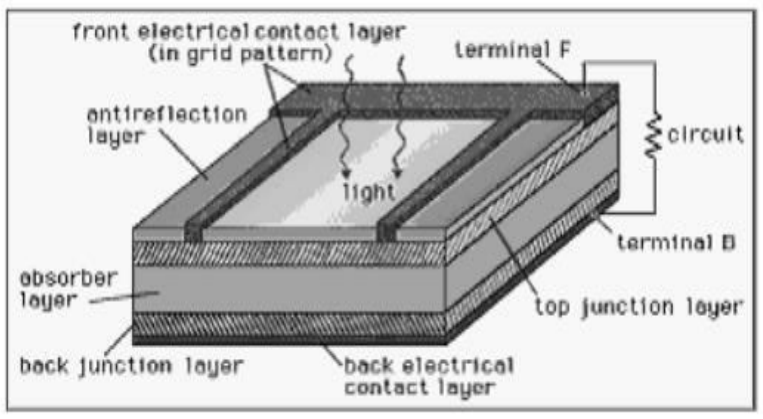

Fig 1.2 Solar Cell

Silicon is used to create the vast majority of solar cells, and as silicon forms vary from amorphous (non-crystalline) to polycrystalline to crystalline (single crystal), the technology is becoming more and more efficient and less expensive. In contrast to batteries or fuel cells, solar cells don't need fuel or rely on chemical processes to generate electricity. Moreover, they are completely mechanically inert, unlike electric generators. By encouraging light transmission to the energy-conversion layers below, the optical coating, also known as the antireflection layer, which reduces light loss via reflection, allows light to enter the device and efficiently traps falling light on the solar cell. Usually created on the cell surface by spin coating or vacuum deposition, the antireflection layer is an oxide of silicon, tantalum, or titanium.

absence of directed direct current. On the other hand, the photovoltaic effect is generated by the introduction of junction-forming layers, which creates an inherent electric field. The electrons that pass through the electrical contact layers and enter an external circuit where they might perform beneficial tasks are, in essence, given collective momentum by the electric field. There are several methods for producing solar cells, and each one has an impact on the cost and efficiency of the final product. These methods include the kind of semiconductor used and the crystal structure utilized. The output of the solar panel is also influenced by other external elements, such as the surrounding weather and its effects on temperature, light, shade, and so on. The goal is to create a system that can maximize power extraction independent of solar cell efficiency or ambient meteorological conditions.

1.2.3 Features of Solar Cells

Determining the maximum power point of a solar cell is challenging due to its non-linear current-to-voltage and power-to-voltage properties. Since maximum power is transmitted at the midway of the current-voltage characteristic, finding the maximum power point on a linear curve is simple. Figure 1.3 depicts a typical V-I characteristic of a solar cell.

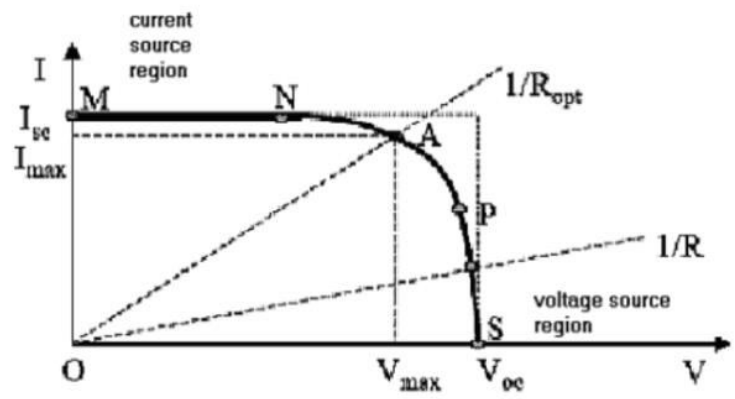

Fig.1.3 Characteristics of Solar Cell

Because of the non-linear connection, one must multiply the output current by the voltage in order to get the maximum power point for a solar cell. The solar cell must always be operated at or very near the location where the product of the output current and voltage is greatest in order to maximize power extraction. The "bend" or "knee" of the I-V characteristic is where this point, also known as the maximum power point (MPP), is situated.

The voltage source area and the current source region make up a solar cell's operational characteristic. Situated on the left side of the current-voltage curve, the current source area is characterized by a high internal impedance of the solar cell. On the right side of the current-voltage curve is the voltage source area, when the internal impedance is low. The characteristic curve shows that the output current is almost constant in the current source area while the terminal voltage fluctuates, and that the terminal voltage varies very little across a large range of output current in the voltage source region.

The maximum power transfer hypothesis states that when the load impedance and the source internal impedance are equal, the power provided to the load reaches its maximum. The impedance seen at the MPPT's input must match the internal impedance of the solar panel in order for the system to function at or near the MPP of the panel. The primary purpose of the MPPT is to modify the solar panel output voltage to a level at which the panel provides the greatest amount of energy to the load, since the impedance observed by the MPPT is a function of voltage (V = I * R). The maximum power operating point is subject to variation due to continually changing environmental circumstances, such as temperature and irradiance, making it difficult to keep the operating point at the maximum power point. As a result, it's critical to continuously monitor the power curve and maintain the working voltage of the solar panel at the highest possible level. The quantity of solar radiation that reaches the earth is known as irradiance, and under perfect circumstances, it is measured near the equator at 1000 W/m2.

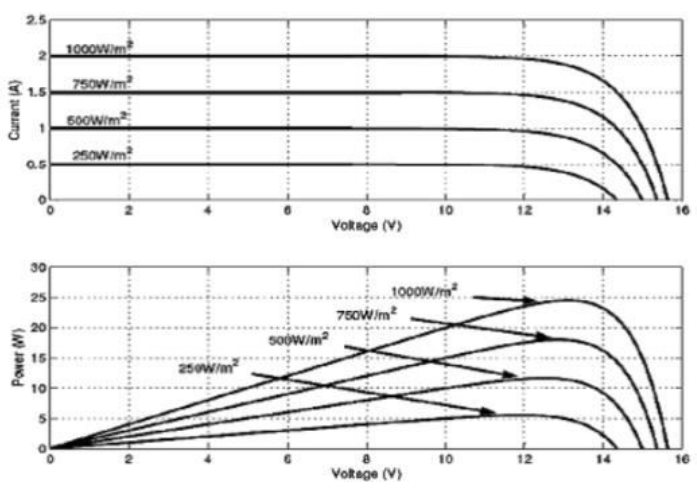

Fig.1.4 I-V and P-V Characteristics of a solar cell for various Irradiance

The orientation and inclination angles of the solar panel have a significant impact on the irradiance at any given location. In northern latitudes, orientation is often assessed with respect to the south; in southern latitudes, it is measured with respect to the north. The inclination angle, on the other hand, is measured with respect to the horizontal. It is possible to calculate the radiation at any place by using these two factors. Information about the irradiance at numerous places throughout the globe is readily accessible. The output power is exactly proportional to the irradiance, as seen in Fig. 2.4. As a consequence, the solar panel will produce less electricity with a lower irradiance. It is also noted, however, that the irradiance has no effect on anything other than the output current. to the semiconductor material's hole and electron mobility. The mobility of electrons and holes in semiconductor materials dramatically decreases with increasing temperature. When the temperature rises to 225ºC, the hole mobility in silicon drops from around 600cm2/volt-sec at 25ºC

to 200cm2/volt-sec. Similarly, the electron mobility in silicon is approximately 1700cm2/volt-sec at 25ºC and will fall to nearly a fourth of this amount. The higher reference temperatures demonstrate that electron and hole mobility decreases with temperature, even if they are not practical working settings for a solar panel.

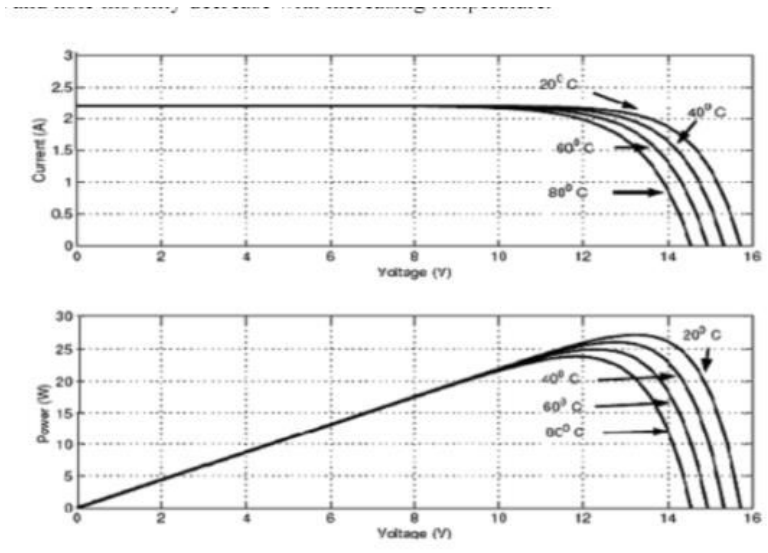

Fig.1.5 I-V and P-V Characteristics of a solar cell with Varying Temperature

In semiconductor materials, temperature also affects the band gap energy. The material's band gap energy will rise in response to a temperature increase. Higher band gap energy means that more photon energy will be needed for the valence band electrons to transition to the conduction band.

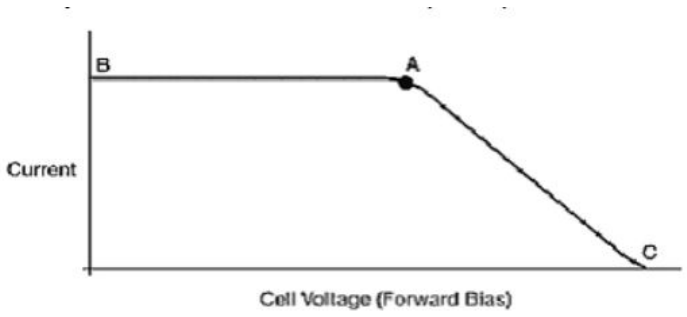

Fig.1.6 Illustration of Maximum Power Point

Point B is where the cell's short circuit current crosses the Y-axis, and Point C is where the cell's open circuit voltage crosses the X-axis. Systems using solar electricity should be built to transmit energy to the load at point A on the I-V curve in order to achieve maximum energy transfer. The majority of the energy should be given as the operating point gets closer to point A, and none at points B or C. It is considerably more crucial that the source and load impedances in a solar panel array match precisely. Cells may be organized into distinct arrays according on their I-V characteristics, and each array can then be optimized to function at its maximum energy transfer point. Because the charged carriers are significantly closer together, the majority of solar cells have high capacitance associated with their forward biased p-n junctions. The unintended capacitance rises with increasing junction area and solar cell size.

The photocurrent IPh, which is directly proportional to the sun irradiance G, is produced by the current source. The solar cell's p-n transition region is analogous to a diode.

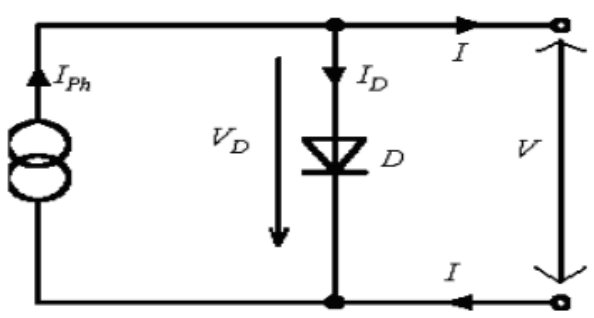

Fig.1.7: Equivalent circuit of a solar cell

The V-I equation of the simplified equivalent circuit could be derived from Kirchhoff's current law

$$I = I_{Ph} - I_D = I_{Ph} - I_S \cdot (\exp(\frac{V}{m \cdot V_T}) - 1)$$

Where Ph I --- Current D photo I --- Diode reverse saturation current m --- Diode current S I --- Ideal diode factor VT is equal to (k*T)/q. temperature (25.7 mV at 25 °C) Temperature Absolute (T) = 1.3824*e-23 * Boltzmann Constant (k) Q equals the electron's charge, or 1.60*e-19 couloumbs. V = the solar cell's output voltage I = the solar cells' output current The electrical process at the solar cell is not best represented by the simple equivalent circuit. It was possible to see a voltage drop in genuine solar cells en route to the exterior connectors. A series resistor, RS, might be used to indicate this voltage loss. In addition, leakage currents were detected, which a parallel resistor RP may explain.

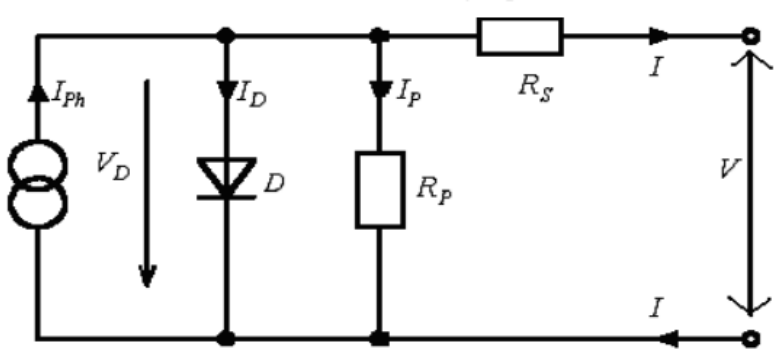

Fig.1.8: Equivalent Circuit for One Diode Model Of A Solar Cell

Derived from Kirchhoff´s first law the equation for the extended I-V curve could be achieved.

$$I = I_{Ph} - I_D - I_P$$

$$I_P = V_D / R_P = \left\{ \frac{(V + IR_S)}{R_P} \right\}$$

$$I = I_{Ph} - \left\{ I_S \left(\exp\left(\frac{q(V + IR_S)}{mkTN_S} \right) - 1 \right) \right\} - \left(\frac{V + IR_S}{R_P} \right)$$

Assuming Ph I to be the photocurrent I stands for diode current. RP is the shunt resistance while RS is the series resistance of the cell. Table 2.1 displays the solar module specs taken from the manufacturer's data sheet.

At Temperature T = 25ºC, Insulation G=1000W/m²		
Open circuit voltage	V_{oc}	21.0 V
Short circuit current	I_{sc}	3.74A
Voltage at max.power	V_m	17.1V
Current at max power	I_m	3.5A
Maximum power	P_m	60.0W

Table 1.1: The key specifications of the solar MSX – 60 PV panel

2. MAXIMUM POWER POINT TRACKING

2.1 Maximum Power Point

Monitoring the Maximum Power Point An electrical system called tracking, also known as MPPT, controls the photovoltaic (PV) modules so they may generate all the electricity they are capable of producing. The modules are not "physically moved" by the MPPT tracking system to aim more directly toward the sun. The completely electronic MPPT system adjusts each module's electrical operating point to enable it to supply the highest amount of power that is possible. Afterwards, more battery charge current is made available by harvesting more power from the modules. While mechanical tracking systems and MPPT may work together, they are entirely separate technologies.

2.1.1 Fractional Open-Circuit Voltage

The approach is predicated on the finding that there is a virtually constant ratio between the array voltage at maximum power (VMPP) and its open circuit voltage (VOC). It has been observed that this factor, k1, ranges from 0.71 to 0.78. After determining the constant k1, VMPP is calculated by regular VOC measurements. Due to the use of erroneous values for the constant k1 in the VMMP calculation, this method's tracking efficiency is rather poor despite its simple and inexpensive implementation.

2.1.2 Fractional Short-Circuit Current

The approach is based on the observation that the PV array's short circuit current (ISC) and current at maximum power point (IMPP) are roughly linearly correlated.

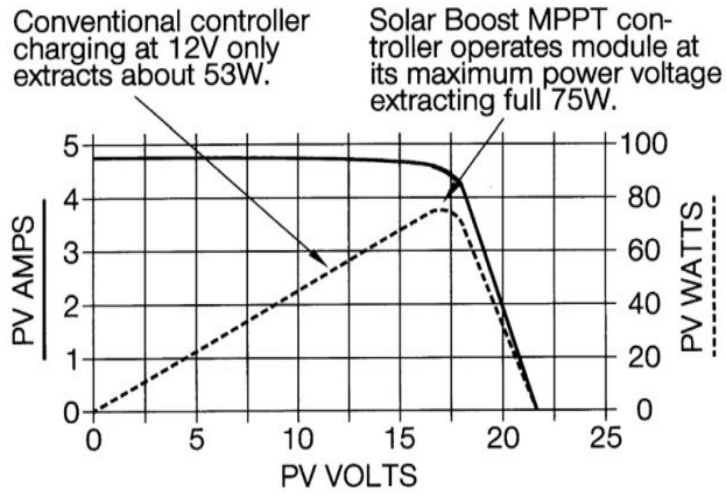

Fig.2.1 PV Characteristics

2.2 INDUCTION MOTOR

2.2.1 Historical Review:

The magnetic effect of an electric current was discovered by Hans Christian Oersted in 1820, which marks the beginning of the history of electrical motors. Michael Faraday created the first crude D.C. motor and found electromagnetic rotation a year later. Faraday later discovered electromagnetic induction in 1831, but Tesla did not create the A.C. asynchronous motor until 1883.

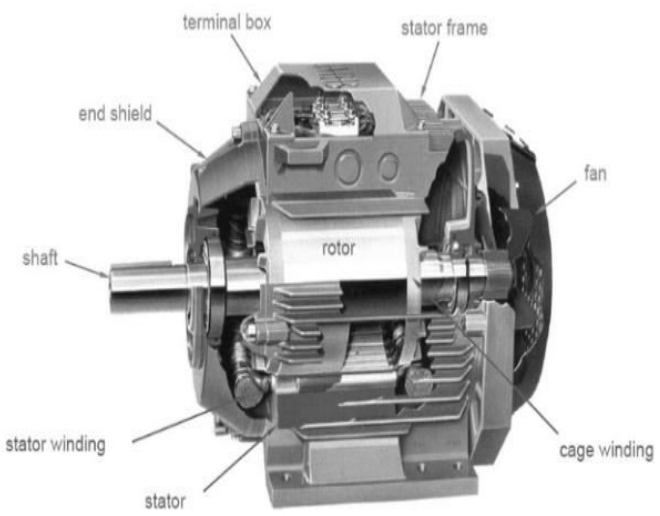

Fig 2.3 Various parts of induction motor

3.MULTI LEVEL INVERTERS

An inverter is an electrical device that changes direct current (DC) into alternating current (AC). By using the proper transformers, switching, and control circuits, the converted AC may be at any desired voltage and frequency. Static inverters are utilized in many different applications, ranging from big electric utility high-voltage direct current applications that transfer bulk power to tiny computer switching power supplies. Static inverters are characterized by their lack of moving components. When supplying AC power from DC sources, such solar panels or batteries, inverters are often used. An electronic oscillator with high power is what the electrical inverter is. The reason for the term "inverted" is because the first mechanical AC to DC converters were designed to operate in reverse, or "inverted," in order to convert DC to AC. The reverse of a rectifier's job is done by an inverter.

3.1 Cascaded H-Bridges inverter

Figure 31.1 shows the single-phase construction of an m-level cascaded inverter. Every individual DC source (SDCS) is linked to a single-phase full-bridge inverter, often known as an H-bridge inverter. By using various combinations of the four switches, S1, S2, S3, and S4, to link the dc source to the ac output, each inverter level may produce one of three voltage outputs: +Vdc, 0Vdc, and –Vdc. Switches S1 and S4 must be switched on in order to acquire +Vdc, whereas switches S2 and S3 must be turned on in order to receive –Vdc. The output voltage is zero when S1 and S2 or S3 and S4 are turned on. The synthesized voltage waveform is equal to the sum of the ac outputs of all the full-bridge inverter levels whose ac outputs are coupled in series.

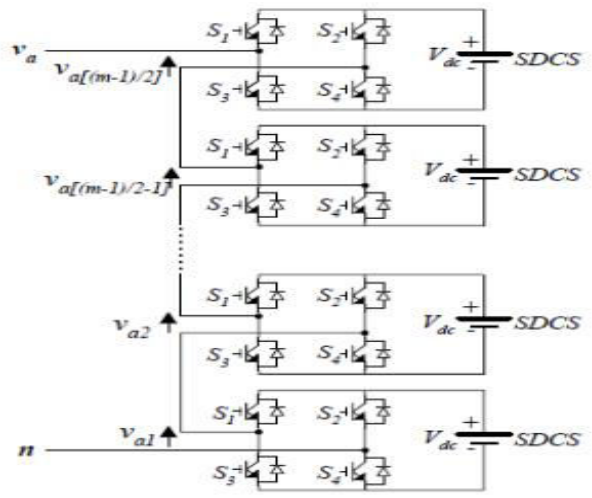

Fig 3.1 Single-phase structure of a multilevel cascaded H-bridges inverter

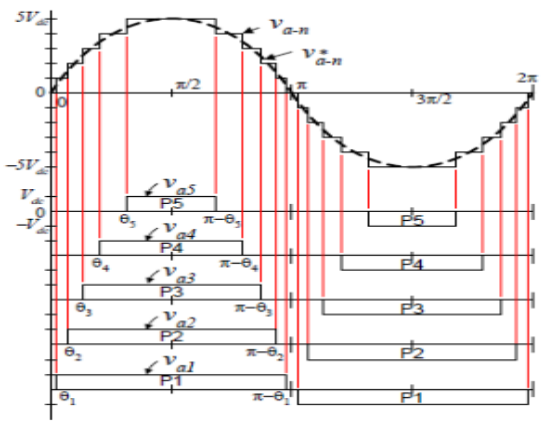

Fig 3.2 Output phase voltage waveform of an 11-level cascade inverter with 5 separate dc sources.

4 .SYSTEM CONFIGURATION AND OPERATION STRATEGRY

4.1 SYSTEM CONFIGURATION

The PV array with a maximum power capacity of 150W at Standard Test Conditions (STC) (1000W/m2 , 25◦C) is considered in accordance with the rating of IM drive coupled water pump. The operating power capacity of the PV array is selected such that it can run the motor pump system with aid of modular multilevel inverter [11], [12].

A. PV ARRAY DESIGN

A 10W solar PV module is made up of 36 cells (36 cells x 0.588 V = 21.6 Voc) connected in series. The specifications are: Maximum power (Pmax) = 10Wp, Voc = 21.6V and Isc = 0.659 A. The maximum voltage and current of a module is Vmp = 17V and Imp = 0.588A (Pmax = Vmp × Imp = 17 × 0.588= 9.96W).

A 20W solar module with 72 cells associated in series is utilized as an input source. The specifications are: Maximum power (Pmax) = 20Wp, Voc = 21.5V and Isc = 1.24 A. The maximum voltage and current ratings of a module at Vmp = 17.5V and Imp =1.143A (Pmax = Vmp × Imp = 17 × 1.14 = 19.38W). The two different ratings of 10W and 20W cited above are connected in series and parallel to achieve the maximum power capacity of 150 W (5 × 10 = 50W, 5 × 20 = 100W) at STC. The current equation of solar cell given in equation (1) has four indefinite constraints (IL, I0, Rs and α) that has to be dogged before attaining the V-I characteristics of the PV cell [13], [14].

$$I = I_L - I_D = I_L - I_0 e^{\left(\frac{V+iRs}{\alpha}\right)} - 1 \qquad (1)$$

1) ESTIMATION OF LIGHT CURRENT (IL)

A scheme to estimate the light current IL is expressed as,

$$I_L = \frac{\varphi}{\varphi_{ref}}[I_{L,ref} + \mu_{I,SC}(T_C - T_{C,ref})] \qquad (2)$$

2) ESTIMATION OF SATURATION CURRENT (I0)

The expression for saturation current is expressed as,

$$I_0 = I_{0,ref}\left(\frac{T_{C,ref}+273}{T_C+273}\right)^3 \exp\left[\frac{e_{gapNs}}{q\alpha_{ref}}\left(1-\frac{T_{C,ref}+273}{T_C+273}\right)\right] \quad (3)$$

During the reference condition the saturation current can be evaluated as,

$$I_{0,ref} = I_{L,ref}\exp\left(-\frac{V_{oc,ref}}{\alpha_{ref}}\right) \quad (4)$$

3) DETERMINATION OF TVTC FACTOR

The Thermal Voltage Timing Completion (TVTC) factor (α) is the task of temperature and expressed as,

$$\alpha_{ref} = \frac{2V_{mp,ref} - V_{oc,ref}}{\frac{I_{sc,ref}}{I_{SC,ref}-I_{mp,ref}} + \ln\left(1-\frac{I_{mp,ref}}{I_{SC,ref}}\right)} \quad (5)$$

$$\alpha = \frac{T_C+273}{T_{C,ref}+273}\alpha_{ref} \quad (6)$$

4) DETERMINATION OF SERIES RESISTANCE (Rs)

The series resistance is determined as,

$$R_S = \frac{\alpha_{ref}\ln\left(1-\frac{I_{mp,ref}}{I_{SC,ref}}\right) + V_{OC,ref} - V_{mp,ref}}{I_{mp,ref}} \quad (7)$$

B. DC-DC CONVERTER DESIGN

An intermediate DC-DC converter in the solar photovoltaic conversion system is set to operate at maximum power for providing symmetric input to MMI. Equation (8) shows the relationship between input voltage and output voltage of DC-DC boost up converter with respect to duty cycle.

$$V_{out} = \frac{V_{in}}{1-D} \quad (8)$$

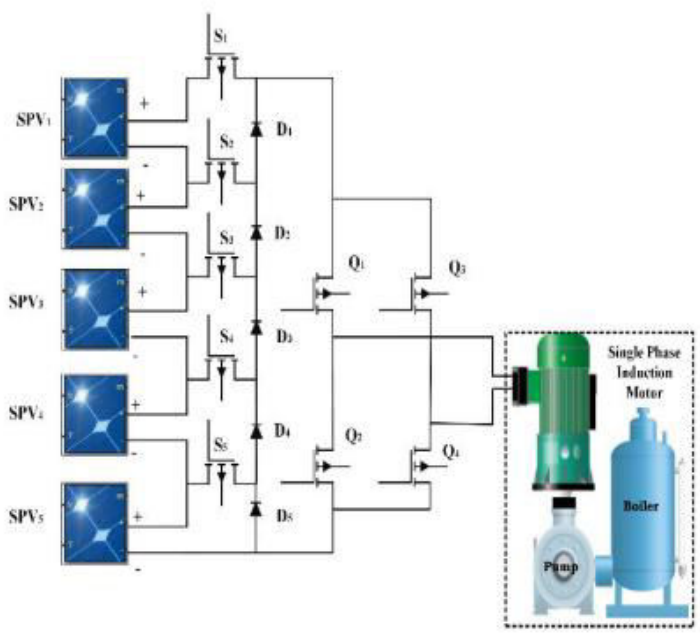

FIGURE4.1. Proposed multilevel inverter.

5.SIMULATION DESIGN AND RESULTS

5.1 SIMULINK MODEL DESIGN

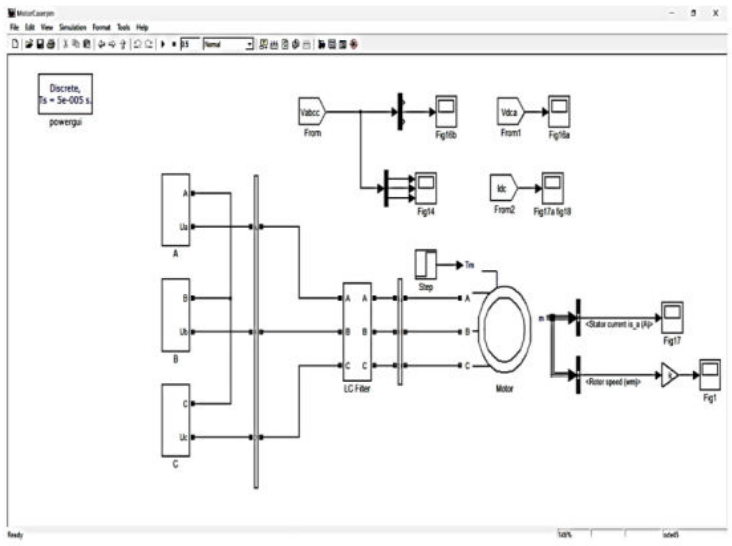

fig 5.1 simulink model design

5.2 SIMULATION RESULTS

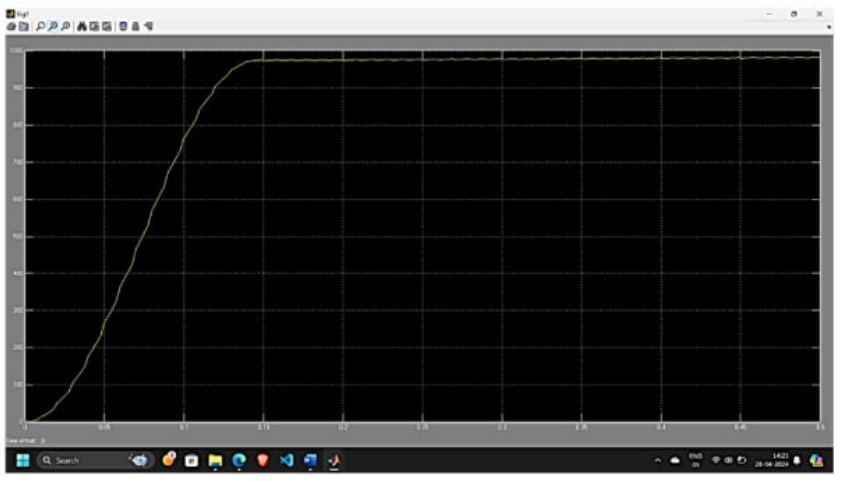

Fig 5.2 Motor Speed

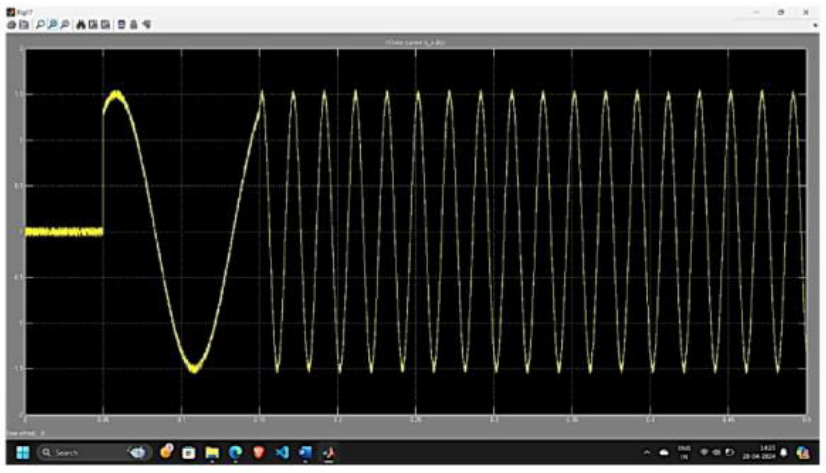

Fig 5.3 Motor Stator Current

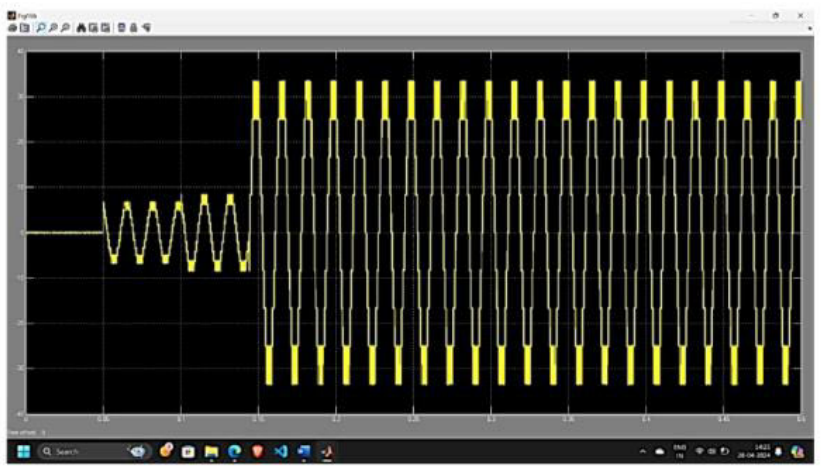

Fig 5.4 AC Output Voltage From Modular Multi Level Inverter

6.CONCLUSION

The proposed work is relevant because it aims to provide the inverter drive with high-quality input power for maritime water pumping applications. In order to determine if a solar PV-fed MMI for induction motor drive speed control is appropriate for a water pumping system meant for maritime applications, both steady state and dynamic behaviors have been studied. After being supplied to an induction motor, the solar PV array is linked to the suggested inverter. The controller receives data on the motor speed in order to provide the best PWM pulses for the inverter switches. With the help of PI and FL based controllers, the motor is started gradually and its speed is raised to reach the reference speed.

Table-6.1 Comparative analysis.

Ref.No	Number of Sources	Number of Switches	Number of Level
18	3n+1	5n+6	6n+3
19	2n+2	4n+6	4n+3
20	4n+2	4n+6	8n+5
21	4n	12n	16n+1
Proposed	**n**	**n+4**	**2n+1**

Both in simulation and experiment, the effectiveness of FL and PI controllers for a workable operation is confirmed, and the outcomes are contrasted. When compared to the PI controller, the findings show that the FL-based controller offers a quicker settling time and fewer harmonics. The suggested control scheme's primary effects are to weaken harmonics at the modular multilevel inverter's output

voltage and lower the induction motor speed control's steady-state inaccuracy. In light of the quantity of components needed for the suggested MMI, Table 3 presents a comparative study of the quantity of semiconductor switches needed for the MMI's design in addition to the inverters found in existing literature. The main parts of a DC microgrid are the controller, load, supply, converter, and grid. A microgrid is often defined as an independent, self-sufficient system that produces electricity for the town and its surrounding areas. The whole DC microgrid component listed is included in the suggested system and works as intended. The future scope is an accurate estimate of power created and electricity utilized.

7.REFERENCES

[1] Received May 27, 2021, accepted June 13, 2021, date of publication June 17, 2021, date of current version June 28, 2021. Digital Object Identifier 10.1109/ACCESS.2021.3090254. Fuzzy Logic Control for Solar PV Fed Modular Multilevel Inverter Towards Marine Water Pumping Applications

[2] H. Lan, Y. Bai, S. Wen, D. C. Yu, Y.-Y. Hong, J. Dai, and P. Cheng, ‘‘Modeling and stability analysis of hybrid PV/diesel/ESS in ship power system,’’ Inventions, vol. 1, no. 5, pp. 1–16, 2016, doi: 10.3390/inventions1010005.

[3] S. G. Jayasinghe, L. Meegahapola, N. Fernando, Z. Jin, and J. M. Guerrero, ‘‘Review of ship microgrids: System architectures, storage technologies and power quality aspects,’’ Inventions, vol. 2, no. 4, pp. 1–19, 2017, doi: 10.3390/inventions2010004.

[4] R. Kumar and B. Singh, ‘‘Single stage solar PV fed brushless DC motor driven water pump,’’ IEEE J. Emerg. Sel. Topics Power Electron., vol. 5, no. 3, pp. 1337–1385, Sep. 2017, doi: 10.1109/JESTPE.2017.2699918.

[5] S. Shukla and B. Singh, ‘‘Single-stage PV array fed speed sensorless vector control of induction motor drive for water pumping,’’ IEEE Trans. Ind. Appl., vol. 54, no. 4, pp. 3575–3585, Jul./Aug. 2018, doi: 10.1109/TIA.2018.2810263.

[6] C.-L. Su, W.-L. Chung, and K.-T. Yu, ‘‘An energy-savings evaluation method for variablefrequency-drive applications on ship central cooling systems,’’ IEEE Trans. Ind. Appl., vol. 50, no. 2, pp. 1286–1297, Mar./Apr. 2014, doi: 10.1109/TIA.2013.2271991.

[7] B. Singh, U. Sharma, and S. Kumar, ‘‘Standalone photovoltaic water pumping system using induction motor drive with reduced sensors,’’ IEEE Trans. Ind. Appl., vol. 54, no. 4, pp. 3645– 3655, Jul./Aug. 2018, doi: 10.1109/TIA.2018.2825285.

[8] A. Dolatabadi and B. Mohammadi-Ivatloo, ‘‘Stochastic risk-constrained optimal sizing for hybrid power system of merchant marine vessels,’’ IEEE Trans. Ind. Informat., vol. 14, no. 12, pp. 5509–5517, Dec. 2018, doi: 10.1109/TII.2018.2824811.

[9] H.-L. Tsai, ‘‘Design and evaluation of a photovoltaic/thermal-assisted heat pump water heating system,’’ Energies, vol. 7, no. 5, pp. 3319–3338, May 2014, doi: 10.3390/en7053319.

[10] M. G. Yu, Y. Nam, Y. Yu, and J. Seo, ‘‘Study on the system design of a solar assisted ground heat pump system using dynamic simulation,’’ Energies, vol. 9, no. 4, pp. 1–17, 2016, doi: 10.3390/en9040291.

[11] S. V. Giannoutsos and S. N. Manias, ‘‘A systematic power-quality assessment and harmonic filter design methodology for variable-frequency drive application in marine vessels,’’ IEEE Trans. Ind. Appl., vol. 51, no. 2, pp. 1909–1919, Mar. 2015, doi: 10.1109/TIA.2014.2347453